Thermal Marangoni instability of a thin film flowing down a thick wall deformed in the backside

L. A. Dávalos-Orozco

Citation: Physics of Fluids **28**, 054103 (2016); doi: 10.1063/1.4948253
View online: http://dx.doi.org/10.1063/1.4948253
View Table of Contents: http://aip.scitation.org/toc/phf/28/5
Published by the American Institute of Physics

PHYSICS OF FLUIDS **28**, 054103 (2016)

Thermal Marangoni instability of a thin film flowing down a thick wall deformed in the backside

L. A. Dávalos-Orozco[a)]
Departamento de Polímeros, Instituto de Investigaciones en Materiales, Universidad Nacional Autónoma de México, Ciudad Universitaria Circuito Exterior S/N, Delegación Coyoacán, México, D.F. 04510, Mexico

(Received 2 December 2015; accepted 15 April 2016; published online 2 May 2016)

The nonlinear instability of a thin liquid film flowing down a heated thick wall with deformations in the backside is investigated. Here it is assumed that the wall deformations are sinusoidal in space. Time dependent perturbations are imposed at the origin of the free surface of the film. It is found that the wall deformations have an important influence on the flow instability. Moreover, it is shown that the free surface has a large amplitude spatial response to the backside deformations of the wall. This response increases its amplitude considerably when decreasing the wall spatial wavelength down to the wavelength of the time dependent perturbations. At that point, numerical analysis reveals that the time dependent perturbations in some cases are almost impossible to observe on the free surface response. However, in other cases, their interaction produces large amplitude nonlinear wave modulations. *Published by AIP Publishing.* [http://dx.doi.org/10.1063/1.4948253]

I. INTRODUCTION

A number of papers have been devoted to the isothermal flow of a thin film flowing down a deformed wall[1–9] under different physical conditions. The case of a heated deformed wall has been investigated in Ref. 10 (Section 5.3) under the small wavenumber lubrication approximation and in Ref. 11 by use of a weighted residuals approach. By means of the same approximation,[12] Ogden *et al*. studied the non-isothermal problem with a porous layer in addition to the liquid layer.

When the problem is non-isothermal, it is important to take into account the thickness and thermal conductivity of the wall in order to model a system which approaches closely to the experiment. In natural convection, the thickness of the wall has been taken into account in Ref. 13, for example. In the case of thermocapillarity, it has been used by Refs. 14–16 and references therein. The deformation of the wall has also been added to a thick wall in the thermal Marangoni problem as in Ref. 17.

The thickness of the wall has been taken into account with topography in the formation of rivulets flowing down an incline in Ref. 18. This and the previous papers were the motivation to investigate in a systematic way the effect of the thickness and thermal conductivity of the wall on the stability of a thin film falling down an incline.[19] Under the small wavenumber approximation, the wall is assumed to be flat in both sides. It is found that the relative thickness and relative thermal conductivity of the wall appear in only one parameter, important enough to determine the Marangoni instability of the flow (see a more general review in Ref. 10). The effect of sinusoidal deformations of a heated thick wall is investigated in Ref. 20. It is found that, under particular conditions, it is possible to decrease the amplitude of the free surface response to the wall deformations increasing the Marangoni number, while the time dependent perturbations imposed on the free surface increase in amplitude, as expected. At the same time, the resonance effect found in Refs. 1 and 2 is able to stabilize in space and time the time dependent perturbations. This surprising result was the incentive to investigate what happens when the wall is cooled from below under similar

a)E-mail: ldavalos@unam.mx

circumstances.[21] It is shown that the free surface response to the wall deformation increases when increasing the magnitude of the negative Marangoni number, while the time dependent perturbations decrease in space and time, as expected. However, it is shown that the resonance effect is more effective to stabilize in space and time than the negative Marangoni numbers used in that paper.

These unforeseen results were an incentive to try to understand the evolution of the nonlinear instability of a thin film flowing down a heated thick wall which has sinusoidal deformations in its backside. The results are presented in this paper under the lubrication approximation.[22,23] Here, the evolution of the thermocapillary perturbations is investigated numerically in space and time.[19–21,24]

The paper is structured as follows. Section II presents the evolution equation of the surface perturbations of a thin film flowing down a heated thick wall with deformations in its backside. Section III shows the numerical results in space and time of the free surface deformation. Sections IV and V are the discussion and conclusions, respectively.

II. EQUATIONS OF MOTION AND THE BENNEY TYPE EQUATION

The evolution of the perturbations on the free surface of a thin film flowing down an inclined heated thick wall with finite thermal conductivity is investigated. It is assumed that the wall has sinusoidal deformations in its backside, that is, the other side with respected to the flat side where the liquid film is flowing down (see Fig. 1).

Use is made of the lubrication approximation where the wavelength of the free surface perturbations is supposed to be very large in comparison with its amplitude and the thickness of the film. In this way, the scaling parameter is $\varepsilon = \frac{2\pi h_0}{\lambda} \ll 1$, where the thickness of the layer is h_0 and λ is the wavelength. Two different scalings are assumed for distance. In the direction perpendicular to the wall, use is made of h_0 and in the direction parallel to it, use is made of $\lambda/2\pi$. Therefore, the scaling representing the variation in different directions is made using ε. Time is made nondimensional with $h_0\lambda/(2\pi\nu)$, velocity with ν/h_0, pressure with $\rho\nu^2/h_0^2$, and temperature with $\triangle T = (T_0 - T_{ambient}) > 0$. Here, ν is the kinematic viscosity and ρ is the density. T_0 is the temperature at the lower face of the wall and $T_{ambient}$ is the temperature of the ambient atmosphere above the fluid free surface.

As can be seen in Fig. 1, the origin is located at the flat side of the wall facing the liquid film. The unperturbed free surface is located at $z = 1$. When time dependent perturbations are imposed on the free surface at $x = 0$, they are located at $z = 1 + H(x, y, t) = h(x, y, t)$. In the present problem, the back face of the wall is located at $z = -d(1 + a_w \sin(q_w x))$ where $d = -d_w/h_0$ and d_w is the dimensional mean thickness of the wall. Notice that the amplitude of the wall backside deformations is restricted to the range $0 \leq a_w < 1$.

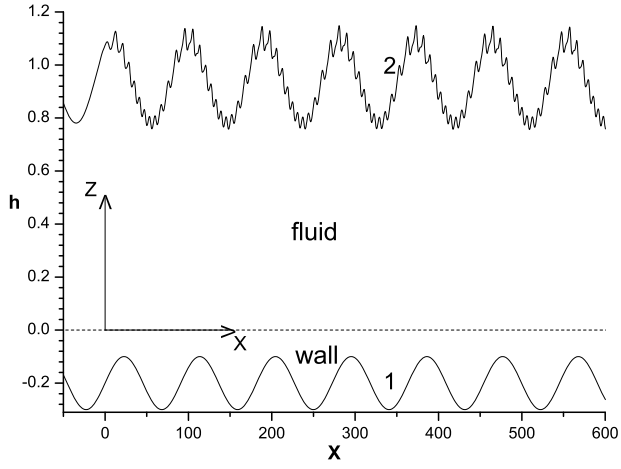

FIG. 1. Sketch of the system. The interface between the fluid and the wall is located at z = 0. (1) Deformation of the wall in its backside. (2) Time dependent perturbations superposed to the response of the free surface due to the backside deformations of the wall.

The following definitions are used. The pressure is p, the velocity components in the (x, y, z) directions are (u, v, w), the temperature of the fluid is T, the temperature of the wall is T_w, the angle of inclination of the wall is β, the Reynolds number is $R = gh_0^3/\nu^2$, the Marangoni number is $Ma = (-d\sigma/dT) \triangle Th_0/(\rho\nu\kappa)$, and the Prandtl number is $Pr = \nu/\kappa$ with κ the heat diffusivity. In this way, the scaled Navier-Stokes, continuity and heat diffusion equations are

$$\varepsilon u_t + \varepsilon u u_x + \varepsilon v u_y + w u_z = -\varepsilon p_x + \varepsilon^2 u_{xx} + \varepsilon^2 u_{yy} + u_{zz} + \mathrm{R}\sin\beta, \tag{1}$$

$$\varepsilon v_t + \varepsilon u v_x + \varepsilon v v_y + w v_z = -\varepsilon p_y + \varepsilon^2 v_{xx} + \varepsilon^2 v_{yy} + v_{zz}, \tag{2}$$

$$\varepsilon w_t + \varepsilon u w_x + \varepsilon v w_y + w w_z = -p_z + \varepsilon^2 w_{xx} + \varepsilon^2 w_{yy} + w_{zz} - \mathrm{R}\cos\beta, \tag{3}$$

$$w_z = -\varepsilon u_x - \varepsilon v_y, \tag{4}$$

$$Pr\left(\varepsilon T_t + \varepsilon u T_x + \varepsilon v T_y + w T_z\right) = \varepsilon^2 T_{xx} + \varepsilon^2 T_{yy} + T_{zz}, \tag{5}$$

$$\frac{Pr}{Q_c}\left(\frac{\rho_w C_{vw}}{\rho C_v}\right)\varepsilon T_{wt} = \varepsilon^2 T_{wxx} + \varepsilon^2 T_{wyy} + T_{wzz}. \tag{6}$$

Eqs. (1)–(3) are the balance of momentum equations and the assumption of fluid incompressibility is given by Eq. (4). The last two Eqs. (5) and (6) correspond to the heat diffusion in the fluid and in the wall, respectively. The small wavenumber approximation is assumed and Eqs. (1)–(6) are scaled by means of the small parameter ε. Subindexes x, y, z, and t mean partial derivatives. Here, the ratio of the wall and fluid heat conductivities is $Q_c = k_w/k_f$. Note that ρ, C_v and ρ_w, C_{vw} are the density and heat capacity of the fluid and the wall, respectively.

A set of boundary conditions have to be determined at different z-positions. At the fluid-wall interface, the velocity satisfies the no-slip condition,

$$u = v = w = 0. \qquad \text{at } z = 0. \tag{7}$$

At the free surface, the normal and shear stresses boundary conditions have to be satisfied. The balance of pressure and surface tension forces on the free surface is represented by the normal stress boundary condition,

$$\begin{aligned} &-p + \frac{1}{N^2}[\varepsilon^3(u_x h_x^2 + v_y h_y^2) + \varepsilon^3(u_y + v_x)h_x h_y - \varepsilon(v_z + \varepsilon w_y)h_y - \varepsilon(u_z + \varepsilon w_x)h_x + w_z] \\ &= P_p(x, y, t) - \frac{3}{N^3}S[(1 + \varepsilon^2 h_y^2)h_{xx} + (1 + \varepsilon^2 h_x^2)h_{yy} - 2\varepsilon^2 h_x h_y h_{xy}]. \quad \text{at } z = h(x, y, t) \end{aligned} \tag{8}$$

where $N = \sqrt{1 + \varepsilon^2 h_x^2 + \varepsilon^2 h_y^2}$. The balance of shear stresses and surface tension temperature gradients on the free surface is represented by the shear stress conditions in two directions,

$$\begin{aligned} &\varepsilon(w_z - \varepsilon u_x)h_x - \frac{1}{2}\varepsilon^2(u_y + v_x)h_y + \frac{1}{2}(u_z + \varepsilon w_x)(1 - \varepsilon^2 h_x^2) \\ &-\frac{1}{2}\varepsilon^2(\varepsilon w_y + v_z)h_x h_y = \frac{Ma}{Pr}(\varepsilon T_x + \varepsilon h_x T_z). \qquad \text{at } z = h(x, y, t) \end{aligned} \tag{9}$$

and

$$\begin{aligned} &\varepsilon(w_z - \varepsilon u_y)h_y - \frac{1}{2}\varepsilon^2(u_y + v_x)h_x + \frac{1}{2}(v_z + \varepsilon w_y)(1 - \varepsilon^2 h_y^2) \\ &-\frac{1}{2}\varepsilon^2(\varepsilon w_x + u_z)h_x h_y = \frac{Ma}{Pr}(\varepsilon T_y + \varepsilon h_y T_z). \qquad \text{at } z = h(x, y, t). \end{aligned} \tag{10}$$

They are the first (Eq. (9)) and second (Eq. (10)) shear stress boundary conditions, respectively. The temperatures of the fluid T and the wall T_w also satisfy conditions at different z-positions. The temperature at the lowest and deformed part of the wall is

$$T_w = 1, \qquad \text{at } z = -d\left(1 + a_w \sin(q_w x)\right). \tag{11}$$

The temperature and heat flux are continuous at the interface of the wall and the fluid,

$$T_w = T \qquad \text{and} \qquad Q_c dT_w/dz = dT/dz \qquad \text{at } z = 0, \tag{12}$$

and a radiation boundary condition is assumed at the free surface,

$$T_z + BiT = 0, \qquad \text{at } z = h(x,y,t). \tag{13}$$

The Biot number is defined as $Bi = H_h h_0/k_f$, where H_h is the coefficient of heat transfer. In the equations the surface tension is assumed to be strong. That is, the nondimensional surface tension number $\Sigma = \sigma h_0/(3\rho\nu^2)$ is changed into $S = \varepsilon^2\Sigma$ with the scaling used.
The kinematic boundary condition is

$$w = \varepsilon h_t + \varepsilon u h_x + \varepsilon v h_y, \qquad \text{at } z = h(x,y,t). \tag{14}$$

This condition physically means that fluid particles always remain at the free surface. In the normal stress boundary condition, an extra term appears representing a pressure which has the form

$$P_p(x,y,t) = A\left|\sin\frac{\omega}{2}t\right|\exp[-a(x^2+y^2)]. \tag{15}$$

It represents a turbulent air jet striking the free surface periodically in order to produce time dependent perturbations which will propagate in space and time in the free surface. Similar stationary jets have been used in real experiments on thin films (see the work of Lacanette *et al.*[25]). The magnitude of the constants selected in Eq. (15) is $A = 0.0001$ and $a = 0.05$. This selection is made in order to attain saturation in the numerical results due to the sensitivity of the system to these two parameters. The absolute value of the sine function is taken because a jet has no suction. In the same way, ω, which represents the frequency of oscillation, is divided by two for that reason.

In order to calculate the evolution equation of the free surface perturbations, the variables are expanded in such a way satisfying the lubrication approximation (small wavenumber approximation) using the small parameter ε as follows:

$$\begin{aligned} &u = u_0 + \varepsilon u_1 + \cdots, && v = v_0 + \varepsilon v_1 + \cdots, && w = \varepsilon(w_1 + \varepsilon w_2 + \cdots),\\ &p = p_0 + \varepsilon p_1 + \cdots, && T = T_0 + \varepsilon T_1 + \cdots, && T_w = T_{w0} + \varepsilon T_{w1} + \cdots. \end{aligned} \tag{16}$$

All the variables depend on (x,y,z,t), but h only depends on (x,y,t). At the lowest order in the expansion, the main flow solutions are

$$p_0 = -(z-h)R\cos\beta - 3S\nabla^2 h + P_p(x,y,t), \tag{17}$$

$$u_0 = -\frac{1}{2}R\sin\beta z(z-2h), \tag{18}$$

$$w_1 = -\frac{1}{2}R\sin\beta z^2 h_x, \tag{19}$$

$$T_0 = \frac{Bi\,[Q_c z + dF(x,y)]}{Q_c(1+Bih(x,y,t)) + BidF(x,y)}, \qquad T_{w0} = \frac{Bi\,[z + dF(x,y)]}{Q_c(1+Bih(x,y,t)) + BidF(x,y)}, \tag{20}$$

where $F(x,y) = F(x) = 1 + a_w\sin(q_w x)$ is the wall backside sinusoidal deformation.

Use of Eqs. (16) and (14) up to first order leads to the evolution equation of the free surface perturbations including the effects of the wall deformations in its backside. That is,

$$h_t + R\sin\beta h^2 h_x + \varepsilon\left\{(R\sin\beta)^2\left(\frac{2}{15}h^6 h_x\right)_x + \frac{1}{3}\nabla\cdot\left[h^3\left(-R\cos\beta\nabla h + 3S\nabla^2\nabla h - \nabla P_p\right) + \frac{1}{2}\frac{Ma}{Pr}\frac{Bih^2}{(1+Bih+Bi\frac{d}{Q_c}F(x,y))^2}\nabla h\right]\right\} = 0. \tag{21}$$

Here $\nabla = (\partial/\partial x, \partial/\partial y)$. When $a_w = 0$, this equation reduces to that of Dávalos-Orozco[19] for a flat thick wall. When $d = 0$ (or else, $Q_c \to \infty$), the equation reduces to that of Joo *et al.*[22,23] in the absence of evaporation. In the isothermal case $Ma = 0$, the equation is the same as that of Dávalos-Orozco *et al.*[24] or that of Joo *et al.*[22] but with $P_p = 0$.

The linear results of Ref. 19 are needed to understand, through the coefficient of the thermocapillary term of Eq. (21), the local behavior of the free surface response to the wall deformation, mainly at the thinnest and at the thickest sections of the wall. Use is made of the same

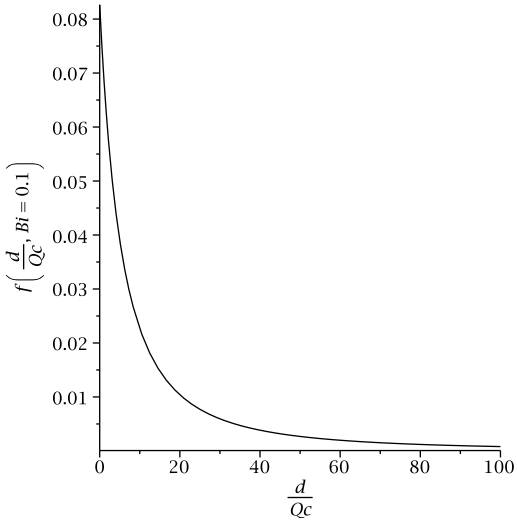

FIG. 2. Plot of the function $f(d/Q_c, Bi) = Bi/(1 + Bi + Bi(d/Q_c))^2$. Here, $Bi = 0.1$ and $f(d/Q_c, Bi = 0.1)$.

magnitudes of all parameters as in Ref. 19 for the sake of comparison in the following figures. Thus, the perturbations start having the same characteristics and will evolve nonlinearly in space and time according to Eq. (21) which includes the effects of the wall deformations. An important function of parameters in Eq. (21) is that corresponding to the thermocapillary term. That is, $f(d/Q_c, Bi) = Bi/(1 + Bi + Bi(d/Q_c))^2$, where $a_w = 0$. This function is shown in a 3D plot in Ref. 19. However, in the present paper the Biot number is fixed at $Bi = 0.1$. Therefore, the plot in Fig. 2 (see Ref. 19) will give us an insight into what is going on when the thickness of the wall varies sinusoidally in space. Due to the presence of the wall deformation in Eq. (21), the parameter in the abscissa of Fig. 2 should be $dF(x)/Q_c$ (instead of d/Q_c), which oscillates with x. Therefore, depending on the x-position, the thermocapillary convection will be more or less effective. For example, the film flowing in the neighborhood of the thinnest section of the wall behaves as expected from the point of view of the coefficient $f(d/Q_c, Bi)$ of the thermocapillary term and plotted in Fig. 2, for given Ma and relative heat conductivity Q_c. That is, at the thinnest section (small d) of the wall, the thermocapillary effects on the free surface of the film are very strong, as shown in the left part of Fig. 2. It is clear in the figure that the function $f(d/Q_c, Bi)$ increases considerably for small wall thicknesses. In contrast, in the thickest section of the wall, the thermocapillary effects are small as observed in the right part of Fig. 2.

III. NUMERICAL ANALYSIS

Here Eq. (21) is solved numerically in space and time using finite differences. The problem is investigated in two dimensions. Some parameters will remain fixed in all the calculations. They are the angle of inclination of the wall $\beta = 90°$ (vertical wall), the expansion parameter $\varepsilon = 0.1$, the Prandtl number $Pr = 7$, and the surface tension number $S = 1$. Notice that the angle of inclination of the wall is selected as $\beta = 90°$ in order to have the most unstable conditions in the instability problem. A parameter is introduced to relate the wavelength of the time dependent perturbations λ with the wavelength of the wall backside deformations $2\pi/q_w$. It is defined as $L = k/q_w$, or in another way, $L = (2\pi/q_w)/\lambda$. In the numerical calculations, use is made of the frequency of the time dependent perturbations applied at $x = 0$ and $z = 1$. Therefore, the definition $\lambda = 2\pi\omega/R$, derived from the phase velocity, is used instead. Therefore, the definition used in practice is $L = R/\omega q_w$. In this way, L expresses the relative magnitudes of k with respect to q_w. As will be shown presently, it plays an very important role in the present problem.

Assuming that $h(x,t) = 1 + H(x,t)$, the initial condition at $t = 0$ (just before time dependent perturbations start to appear), the free surface has the height $z = h(x,t) = 1$ and $H(x,t) = 0$. The

boundary conditions are the following. At x = −100 and x = RT + 100, the perturbation satisfies $H(x,t) = dH(x,t)/dx = 0$, where $t = T$ is the time interval of propagation of the perturbation which runs with a phase velocity R. In this way, when $t > 0$, the free surface starts to respond to the backside wall deformations and at $x = 0$, it is subjected to periodic time dependent perturbations.

Notice that only four figures are presented. Two of them correspond to Marangoni number Ma = 50 and the other two to Ma = 100. The first one of each pair is for a small Reynolds number and the second one is for a large Reynolds number. In each figure, the results are presented in such a way that graphics corresponding to different parameters may be compared to each other using the scaling of the vertical axis. Figure (a) corresponds to $d/Q_C = 1$ and figure (b) to $d/Q_C = 10$. Then, each sub-figure (a) and (b) presents results for wall deformation amplitudes $a_w = 0.5$ and $a_w = 0.9$. In this way, it is possible to see a wide map of the behavior of the thin film stability.

It is important to point out that the graph of each free surface deformation has a mean position at $z = 1$. However, notice that the figures contain a number of ordered graphs which are plotted very near to each other. This is done for the sake of presentation and comparison of the results for different magnitudes of the parameters.

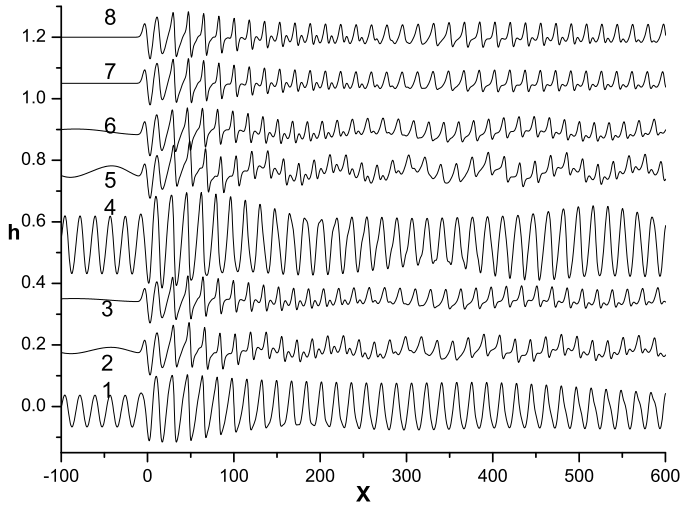

(a)

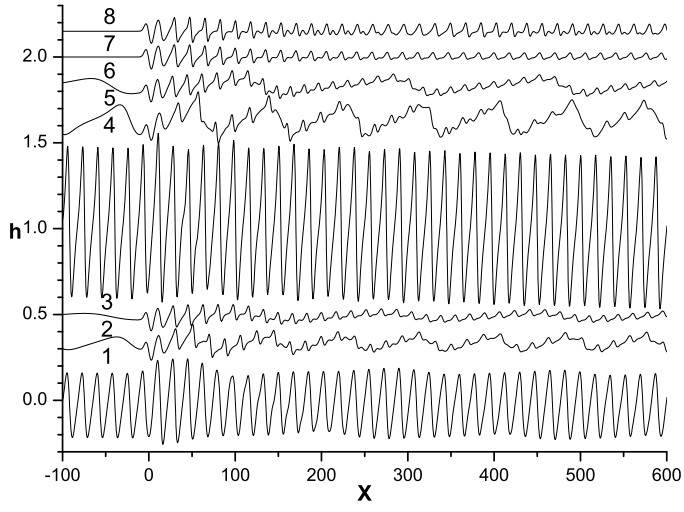

(b)

FIG. 3. Time = 1000. $Ma = 50$, $\omega = 0.5$, $R = 1.391$. Fig. 3(a): $d/Q_c = 1$ and Fig. 3(b): $d/Q_c = 10$. $a_w = 0.5$: (1) $L = 1$, (2) $L = 5$, (3) $L = 10$, $a_w = 0.9$: (4) $L = 1$, (5) $L = 5$, (6) $L = 10$, (7) Ref. 19, (8) fixed temperature $d/Q_c = 0$. The pure response is from $x = -100$ to 0.

Therefore, the results are calculated for two magnitudes of the Marangoni number $Ma = 50$ and 100. Figure 3 for Ma = 50 shows some samples for $\omega = 0.5$ and Reynolds number $R = 1.391$. The figure is structured in such a way that it is possible to compare the behavior of the free surface response to the wall deformations (see the region x = −100 to 0) and the time dependent perturbations under different geometric conditions of the wall. Figs. 3(a) and 3(b) show results for $d/Q_c = 1$ and 10, respectively. Besides, Figs. 3(a) and 3(b) are divided into different sections for the sake of comparison. First, for the deformation amplitude $a_w = 0.5$, curves (1)–(3) correspond to $L = 1$, 5, and 10, respectively. Second, for $a_w = 0.9$, curves (4)–(6) correspond to $L = 1$, 5, and 10, respectively. Third, it is of interest to compare the present results with those of Dávalos-Orozco[19] (curve 7) with a thick flat wall for the same corresponding d/Q_c and with those of a very thin or very good conducting flat wall (curve 8), calculated here in space and time.

It is convenient to start from curves 8 and 7 in Fig. 3(a) for $d/Q_c = 1$. Note that the amplitude of curve 7 is smaller than that of curve 8 due to the presence of d/Q_c which represents a thick wall with finite thermal conductivity. The geometry of the wall appears when $a_w > 0$. For $a_w = 0.5$, it is clear that the amplitude of the free surface response (see x = −100 to 0) increases decreasing

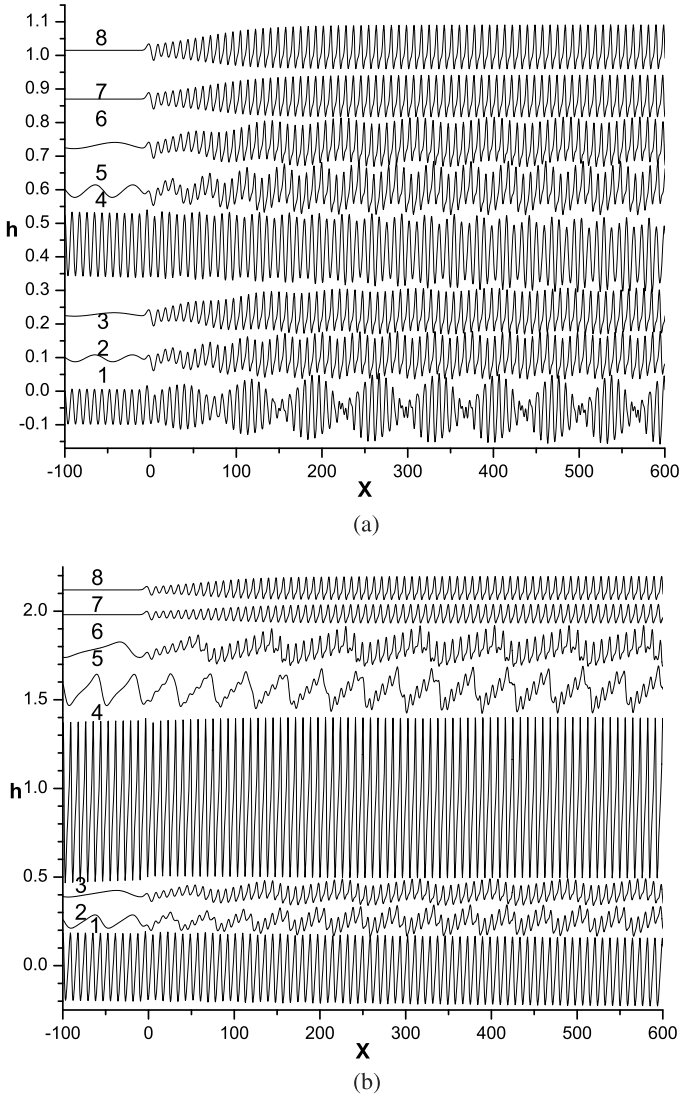

FIG. 4. Time = 600. $Ma = 50$, $\omega = 2$, $R = 2.783$. Fig. 4(a): $d/Q_c = 1$ and Fig. 4(b): $d/Q_c = 10$. $a_w = 0.5$: (1) $L = 1$, (2) $L = 5$, (3) $L = 10$, $a_w = 0.9$: (4) $L = 1$, (5) $L = 5$, (6) $L = 10$, (7) Ref. 19, (8) fixed temperature $d/Q_c = 0$. The pure response is from $x = -100$ to 0.

the magnitude of L (from curves 3 to 1). Observe that the time dependent perturbations superpose nonlinearly to the free surface response. Even more, as can be seen in curve 1, superposition leads to a strong wave modulation due to the similarity of the two wavelengths λ and $2\pi/q_w$.

Other results are found for a larger wall amplitude when $a_w = 0.9$. Note that in this case the resonant amplitude is larger than before when going from $L = 10$ (curve 6) to $L = 1$ (curve 4). Clearly, the amplitude of curve 4 is larger than that of curve 1. Decreasing the parameter to the magnitude $L = 1$ it is shown that the time dependent perturbations merge with the free surface response in such a way that it is not possible to distinguish them in the first units in space. Afterwards, it is possible to observe a mild space modulation. Here, the amplitude of the free surface response behaves in a similar way to the resonance effect found in other papers.[1,26,27]

In Fig. 3(b) the results for $d/Q_c = 10$ are shown. The amplitude of curve 7 is now notably smaller than that of curve 8 due to the increase of d/Q_c. For $a_w = 0.5$, the free surface response can be seen in the range x = −100 to 0. The decrease of L from curves 3 to 1 produces an increase of the response in comparison with Fig. 3(a). When $a_w = 0.9$ the resonance is more important and the amplitude of curve 4 is very large in comparison with that of Fig. 3(a). Again, it is not possible

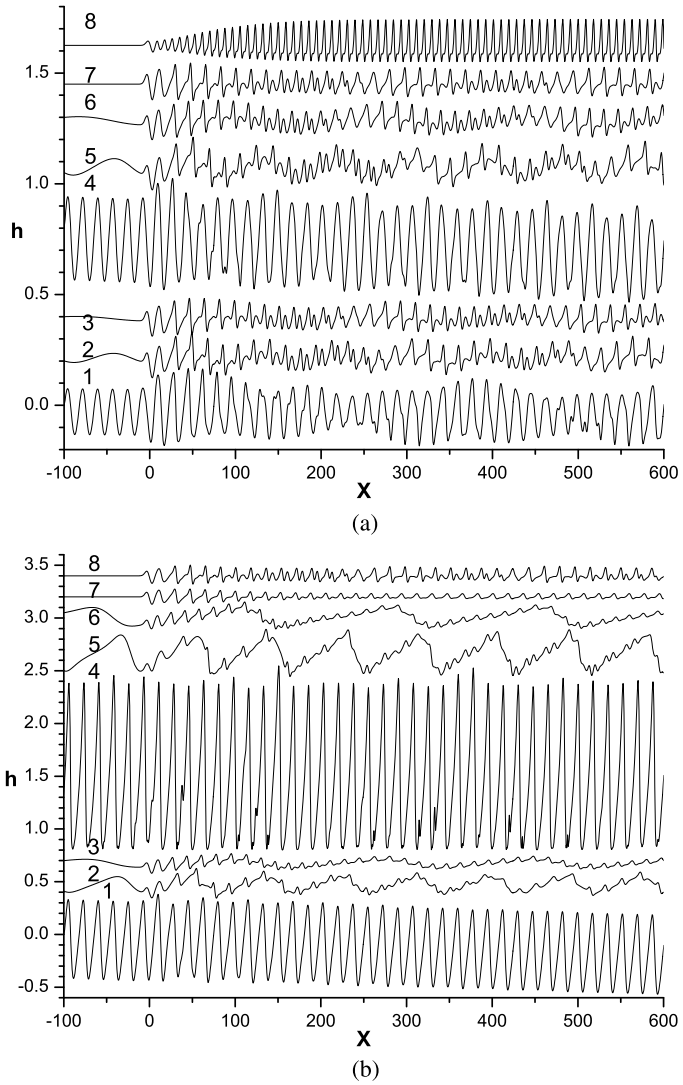

FIG. 5. Time = 1000. $Ma = 100$, $\omega = 0.5$, $R = 1.391$. Fig. 5(a): $d/Q_c = 1$ and Fig. 5(b): $d/Q_c = 10$. $a_w = 0.5$: (1) $L = 1$, (2) $L = 5$, (3) $L = 10$, $a_w = 0.9$: (4) $L = 1$, (5) $L = 5$, (6) $L = 10$, (7) Ref. 19, (8) fixed temperature $d/Q_c = 0$. The pure response is from $x = -100$ to 0.

to distinguish the time dependent perturbations when $L = 1$ in curve 4 but there is a visible wave modulation in curve 1 as a consequence of the nonlinear interaction between the response and the time dependent perturbations. The very large amplitude of the response hides the time dependent perturbations in curve 4.

The results of Fig. 4 for $Ma = 50$ correspond to a higher Reynolds number $R = 2.783$. In Fig. 4(a) for $d/Q_c = 1$, it is interesting the way the free surface perturbations present the wave modulation for $a_w = 0.5$ and 0.9. The reason is the decrease of the wavenumber of the time dependent perturbations. This modulation is remarkable at resonance for $L = 1$ in curves 1 and 4. In the case $a_w = 0.9$ the strong increase in amplitude of curve 4 hides the small wave modulation. In Fig. 4(b) for $d/Q_c = 10$ the increase in amplitude at resonance ($L = 1$) is more impressive. It shows no clear modulation at all in curve 1 and curve 4 hiding the time dependent perturbations. Notice the different response of the free surface in curves 5 and 6 of this figure in comparison with the corresponding ones of Fig. 4(a). A similar result is found in curves 5 and 6 in the previous and following figures.

It is well known that an increase of the Marangoni number destabilizes the free surface perturbations. This has as consequence an increase in amplitude. The Marangoni number is duplicated in

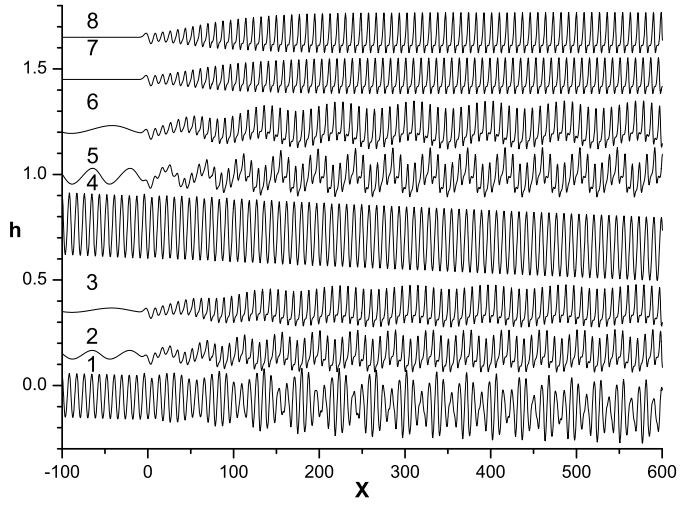

(a)

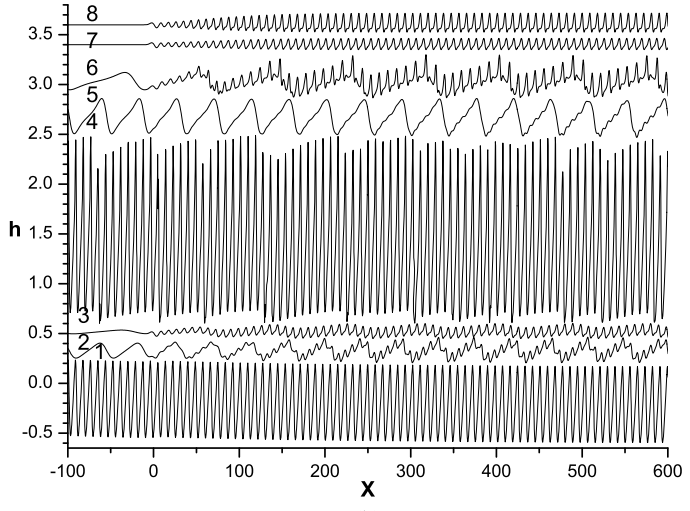

(b)

FIG. 6. Time = 600. $Ma = 100$, $\omega = 2$, $R = 2.783$. Fig. 6(a): $d/Q_c = 1$ and Fig. 6(b): $d/Q_c = 10$. $a_w = 0.5$: (1) $L = 1$, (2) $L = 5$, (3) $L = 10$, $a_w = 0.9$: (4) $L = 1$, (5) $L = 5$, (6) $L = 10$, (7) Ref. 19, (8) fixed temperature $d/Q_c = 0$. The pure response is from $x = -100$ to 0.

the following figures up to $Ma = 100$. Notice that the amplitudes in curves 8 of Figs. 5(a) and 5(b) have increased. In comparison with curves 8, an important decrease in amplitude is found in curve 7 of Fig. 5(a) for $d/Q_c = 1$ and in curve 7 for $d/Q_c = 10$ in Fig. 5(b).

The frequency and Reynolds number of Fig. 5 are $\omega = 0.5$ and $R = 1.391$. With the present Reynolds and Marangoni numbers, the response of the free surface has a larger amplitude as can be seen in the curve 4 of Fig. 5(a) in comparison with curve 4 of Fig. 3(a). This has important consequences in the behavior of the time dependent perturbations, mainly in the way they superpose nonlinearly to the response. However, in this case too, it is possible to have a resonant effect when decreasing the parameter L from 10 to 1. Compare the envelops of the modulation found in curves 4 and 1 of Figs. 3(a) and 5(a). Furthermore, the amplitude of the response at resonance of curves 4 and 1 in Fig. 5(b), for $d/Q_c = 10$, is still more larger than that of Fig. 5(a). Moreover, they have almost twice the amplitude as those of Fig. 3(b). However, here the modulation is barely seen.

The Reynolds number is increased to $R = 2.783$ in Fig. 6 with $\omega = 2$ and $Ma = 100$. The differences in the wavenumber of the time dependent perturbations are clearly seen. The free surface response differs from those of the previous figure but it is similar to that of Fig. 4 except for the amplitude. For example, when resonance is important in curves 4 and 1, the amplitude is almost twice that of Fig. 4. Therefore, the increase in Marangoni number produced an increase in amplitude both in the response and in the time dependent perturbations. A comparison of the curves in this Fig. 6 shows that the increase of d/Q_c from 1 to 10 increases considerably the amplitude of the response at $L = 1$. In fact, curve 4 of Fig. 6(b) has an amplitude more than five times larger than the corresponding one of Fig. 6(a) and curve 1 of Fig. 6(b) is three times larger in amplitude than the corresponding one of Fig. 6(a). These results show the importance of all the parameters involved in the present problem.

IV. DISCUSSION

The resonant effect shows a significant amplitude increase of the response of the free surface to the wall deformations in its backside. From the point of view of the evolution equation, this result is similar to that found when the deformations of the wall are located in the side of the liquid film. In the present problem, Eq. (21) has the algebraic expression for the deformation of the wall in the denominator of the thermocapillary term. When the deformations are located at the wall-liquid interface, in the isothermal case,[1] the expression of the deformation appears in the numerator of the capillary term. Therefore, linearizing that equation,[1,9] it is possible to verify that the wall deformation appears as a spatial periodic forcing term. As a consequence, it is possible to have resonance in space and time for some relative magnitudes of the wavelengths of the time dependent perturbations and the wall deformation, that is, at some magnitude of L. The same has been found in the lubrication approximation when the wall is very thin and very good heat conductor (see Ref. 10 Section 5.3). However, when the wall is thick and has finite thermal conductivity,[20,21] the expression of the wall deformation appears both in the capillary term and in the numerator and denominator of the thermocapillary term.

In the present problem, the algebraic expression of the wall deformation only appears in the denominator of the thermocapillary term. This is because the deformation does not affect the liquid film flow directly as in the previous cases. It only affects the flow by thermal effects. Therefore it of interest to ask why it is also possible to have free surface response resonance as in the other papers. The answer is that this thermocapillary term has to be derivated by the spatial nabla operator applied outside the brackets in Eq. (21). This operation allows the expression of the wall deformation to appear in the numerator of a new term which, under particular conditions, makes it possible to have a very large amplitude of the free surface response. In other words, it is able to appear as a spatial forcing term. Here, as in previous papers, those conditions are measured by means of L, as can be seen in all the figures presented in this paper. Therefore, this resonance appears in a variety of ways, depending on the different magnitudes of the large number of parameters of the problem. It is clear that, in order to have this large variety of phenomena, it is of particular importance the nonlinear interaction between the free surface response and the time dependent perturbations.

V. CONCLUSIONS

The influence of wall backside deformations on the thin film instability has been investigated in this paper. It is shown that the change of the different parameters of the problem produces a variety of results due to the nonlinear interaction of the free surface response to the wall deformation and the free surface time dependent perturbations.

Some sample results are presented in the figures. They show the relevance the parameter d/Q_c[19–21] has in the present problem. Notice that this parameter plays the role of the effective importance of the wall deformation. However, a_w and q_w are crucial to attain a resonant effect. Observe in the figures that the amplitude of the free surface response depends strongly on the a_w. The reason is that when this amplitude a_w is large but smaller than one, there is a region where the wall is very thin. Therefore, in this section, the liquid film feels the wall as a very good conductor. The sudden change of relative high thermal conductivity produces a large bump in the free surface response as found in experiments with a small area hot plate located in the wall.[28–31] This effect is reinforced by the wavenumber q_w of the wall deformation which leads to resonance when L decreases.

The results are validated in all the figures by means of the curve 7 which is calculated numerically with Eq. (21) in the case of zero wall deformation, that is, $a_w = 0$. It is shown that this curve 7 is the same as the corresponding one in Ref. 19 for a flat wall.

Besides, the validation with respect to experimental results is explained by means of Refs. 28–31 where the flow down a wall with a finite hot plate is investigated. Those experiments show that when the thin film runs into a hot plate, the free surface shows a very high bump. This occurs as a result of the sudden and large change of the temperature of the wall, which is traduced into a sudden and large thermal change in the surface tension, affecting strongly the amplitude of the free surface response.

In this way, it is shown in the paper that it is also possible to have a large sudden change in thermocapillary effects by increasing the amplitude of the sinusoidal wall deformation and reducing its wavelength (which is similar to decreasing L). For this reason, the free surface response is able to show a large amplitude (resonance) when the thermocapillary effects are important (see Fig. 2). This occurs just when the wall thickness is very small (see the coefficient $\mathrm{f}(\mathrm{d}/Q_C, \mathrm{Bi})$ of the thermocapillary term in Fig. 2 for small d/Q_C). Therefore, it is demonstrated that when the thermocapillary coefficient $\mathrm{f}(\mathrm{d}/Q_C, \mathrm{Bi})$ presents a large sudden change in Eq. (21), the amplitude of the free surface response is very large.

The results presented above show the importance the wall deformations have on the thin film instability even when they appear in the backside. That is why care should be taken too when inserting in the wall equipment to measure non-isothermal phenomena in thin liquid films. Those elements change the local thickness and local thermal conductivity of the wall and, depending on the subject of research, they may have significant consequences on the experimental results.

ACKNOWLEDGMENTS

The author would like to thank Alberto López, Caín González, Raúl Reyes, Ma. Teresa Vázquez, and Oralia Jiménez for technical support.

[1] L. A. Dávalos-Orozco, "Nonlinear instability of a thin film flowing down a smoothly deformed surface," Phys. Fluids **19**, 074103 (2007).
[2] L. A. Dávalos-Orozco, "Instability of thin films flowing down flat and smoothly deformed walls," Microgravity Sci. Technol. **20**(3-4), 225-229 (2008).
[3] S. Veremieiev, H. M. Thompson, M. Scholle, Y. C. Lee, and P. H. Gaskell, "Electrified thin film flow at finite Reynolds number on planar substrates featuring topography," Int. J. Multiphase Flow **44**, 48-69 (2012).
[4] T. Pollak and N. Aksel, "Crucial flow stabilization and multiple instability branches of gravity-driven films over topography," Phys. Fluids **25**, 024103 (2013).
[5] C. Li, J. Pei, and X. Ye, "Spreading of droplet with insoluble surfactant on corrugated topography," Phys. Fluids **26**, 092103 (2014).
[6] C. Ketelaar, "Stability of electrolyte films on structured surfaces," Interfacial Phenom. Heat Transfer **2**, 181-198 (2014).
[7] Y. Trifonov, "Stability of a film flowing down an inclined corrugated plate: The direct Navier-Stokes computations and Floquet theory," Phys. Fluids **26**, 114101 (2014).
[8] M. Schorner, D. Reck, and N. And Aksel, "Does the topography's specific shape matter in general for stability of film flows," Phys. Fluids **27**, 042103 (2015).

[9] L. A. Dávalos-Orozco, "Stability of thin viscoelastic films falling down wavy walls," Interfacial Phenom. Heat Transfer **1**, 301-315 (2013).
[10] L. A. Dávalos-Orozco, "Stability of thin liquid films falling down isothermal and nonisothermal walls," Interfacial Phenom. Heat Transfer **1**, 98-138 (2013).
[11] S. J. D'Alessio, J. P. Pascal, H. A. Jasmine, and K. A. Ogden, "Film flow over heated wavy inclined surfaces," J. Fluid Mech. **665**, 418-456 (2010).
[12] K. A. Ogden, S. J. D. D'Alessio, and J. P. Pascal, "Gravity-driven flow over heated, porous, wavy surfaces," Phys. Fluids **23**, 122102 (2011).
[13] I. Pérez-Reyes and L. A. Dávalos-Orozco, "Effect of thermal conductivity and thickness of the walls in the convection of a viscoelastic Maxwell fluid layer," Int. J. Heat Mass Transfer **54**, 5020-5029 (2011).
[14] A. Oron, S. G. Bankoff, and S. H. Davis, "Thermal singularities in film rupture," Phys. Fluids **8**, 3433-3435 (1996).
[15] T. Gambaryan-Roisman, "Marangoni convection, evaporation and interface deformation in liquid films on heated substrates with non-uniform thermal conductivity," Int. J. Heat Mass Transfer **53**, 390-402 (2010).
[16] I. J. Hernández Hernández and L. A. Dávalos-Orozco, "Competition between stationary and oscillatory viscoelastic thermocapillary convection of a film coating a thick wall," Int. J. Therm. Sci. **89**, 164-173 (2015).
[17] Yu. O. Kabova, A. Alexeev, T. Gambarian-Roisman, and P. Stephan, "Marangoni-induced deformation and rupture of a liquid film on a heated microstructured wall," Phys. Fluids **18**, 012104 (2006).
[18] T. Gambaryan-Roisman and P. Stephan, "Flow and stability of rivulets on heated surfaces with topography," J. Heat Transfer **131**, 033101 (2010).
[19] L. A. Dávalos-Orozco, "The effect of the thermal conductivity and thickness of the wall on the nonlinear instability of a thin film flowing down an incline," Int. J. Non-Linear Mech. **47**, 1-7 (2012).
[20] L. A. Dávalos-Orozco, "Non linear instability of a thin film flowing down a smoothly deformed thick wall of finite thermal conductivity," Interfacial Phenom. Heat Transfer **2**, 55-74 (2014).
[21] L. A. Dávalos-Orozco, "Non linear instability of a thin film flowing down a cooled wavy thick wall of finite thermal conductivity," Phys. Lett. A **379**, 962-967 (2015).
[22] S. W. Joo, S. H. Davis, and S. G. Bankoff, "Long-wave instabilities of heated falling films: Two-dimensional theory of uniform layers," J. Fluid Mech. **230**, 117-146 (1991).
[23] S. W. Joo and S. H. Davis, "Instabilities of three-dimensional viscous falling films," J. Fluid Mech. **242**, 529-547 (1992).
[24] L. A. Dávalos-Orozco, S. H. Davis, and S. G. Bankoff, "Nonlinear instability of a fluid layer flowing down a vertical wall under imposed time-periodic perturbations," Phys. Rev. E **55**, 374-380 (1997).
[25] D. Lacanette, A. Gosset, S. Vincent, J.-M. Buchlin, and E. Arquis, "Macroscopic analysis of gas-jet wiping: Numerical simulation and experimental approach," Phys. Fluids **18**, 042103 (2006).
[26] Y. Y. Trifonov, "Stability and nonlinear wavy regimes in downward film flows on a corrugated surface," J. Appl. Mech. Tech. Phys. **48**, 91-100 (2007).
[27] Y. Y. Trifonov, "Stability of a viscous liquid film flowing down a periodic surface," Int. J. Multiphase Flow **33**, 1186-1204 (2007).
[28] A. M. Frank and O. A. Kabov, "Thermocapillary structure formation in a falling films: Experiment and calculations," Phys. Fluids **18**, 032107 (2006).
[29] N. Tiwari, Z. Mester, and J. M. Davis, "Stability and transient dynamics of thin liquid films flowing over locally heated surfaces," Phys. Rev. E **76**, 056306 (2007).
[30] E. A. Chinnov and E. N. Shatskii, "Effect of thermocapillary perturbations on the wave motion in heated falling liquid film," Tech. Phys. Lett. **36**, 53-56 (2010).
[31] Yu. Kabova, V. V. Kuznetsov, O. Kabov, T. Gambaryan-Roisman, and P. Stephan, "Evaporation of a thin viscous liquid film shared by gas in microchannels," Int. J. Heat Mass Transfer **68**, 527-541 (2014).